International Journal of Nanomedicine

Dovepress
open access to scientific and medical research

Open Access Full Text Article

ORIGINAL RESEARCH

Pulmonary deregulation of expression of *miR-155* and two of its putative target genes; *PROS1* and *TP53INP1* associated with gold nanoparticles (AuNPs) administration in rat

This article was published in the following Dove Press journal:
International Journal of Nanomedicine

Ghada E Ali[1]
Marwa A Ibrahim[1]
Ayman H El-Deeb[2]
Hassan Amer[1]
Said M Zaki[1]

[1]Cairo University, Faculty of Veterinary Medicine, Department of Biochemistry and Chemistry of Nutrition, Giza 12211, Egypt; [2]Cairo University, Faculty of Veterinary Medicine, Department of Virology, Giza 12211, Egypt

Background: Gold nanoparticles (AuNPs) have been considered as an ideal candidate in various biomedical applications due to their ease of tailoring into different size, shape, and decorations with different functionalities. The current study was conducted to investigate the epigenetic alteration in the lung in response to AuNPs administration regarding microRNA-155 (miR-155) gene which can be involved in AuNP-induced lung pathogenesis.

Methods: Thirty-two Wister rats were divided into two equal groups, control group and AuNPs treated group which received a single intravenous (IV) injection of plain spherical AuNPs (0.015 mg/kg body wt) with an average diameter size of 25±3 nm. Lung samples were collected from both the control and injected groups at one day, one week, one month and two months post-injection. The alteration of relative expression of *miR-155* gene and two of its putative target genes; tumor protein 53 inducible nuclear protein 1 *(TP53INP1)* and protein *S (PROS1)* was investigated by real time PCR and protein S (PS) expression was analyzed by Western blotting technique.

Results: The obtained results revealed that AuNPs administration significantly increases the expression level of *miR-155* and reduce relative mRNA expression of *TP53INP1* and *PROS1* genes at one day post-injection. In contrast, a significant down-regulation of *miR-155* level of expression concurrent with up-regulation of expression level of *TP53INP1* and *PROS1* genes were shown at one week, one month and two months post-injection. PS levels were mirrored to their *PROS1* mRNA levels except for two month post-injection time point.

Conclusions: These findings indicate epigenetic modulation in the lung in response to AuNPs administration regarding the *miR-155* gene which can be involved in AuNP-induced lung pathogenesis.

Keywords: AuNPs, MiR-155, epigenetic, PROS1, TP53INP1

Introduction

Nanomedicine is a rapidly growing vital field that aims to use various nanomaterials (NMs) to tackle a range of biomedical applications and medical ailments.[1] Metallic NMs constitute promising platforms for various purposes due to their peculiar photonic, electronic, catalytic, and therapeutic properties, easy surface functionalization and versatile methods of synthesis ensuring wide size and shape features.[2] Among them, AuNPs have attracted wide attention in various biomedical applications due to the unique properties that make them superior over other nanoparticles. These distinctive features include their photoactivation capability, inertness, biocompatibility, and their relatively simple

Correspondence: Ghada E Ali
14A Selim-street King Faisal St.
Cairo University, Giza, Egypt
Tel +20 114 290 2365
Email dr.ghadaalimg@gmail.com

submit your manuscript | www.dovepress.com
DovePress
http://doi.org/10.2147/IJN.S208372

generation and surface modification.[3] Moreover, they have an exceptional electric and magnetic properties which make them an ideal candidate in the field of biological tagging, chemical and biological sensing, optoelectronics, photothermal therapy, biomedical imaging, DNA labeling, gene therapy, microscopy and photoacoustic imaging, surface-enhanced Raman spectroscopy, tracking and drug delivery, catalysis and cancer therapy.[4]

The potential health risk following the NMs therapeutic or diagnostic application is becoming more controversial. In addition to genotoxicity, mutagenicity, oxidative stress and inflammation, nanotoxicity can also be mediated by epigenetic modifications that may contribute to adverse health effects and can play a potential causative role in the pathogenesis of many diseases including cancer.[5] Therefore, more research has recently raised a concern about possible epigenetic toxicity and health effects induced by NMs.[3,6,7] Whilst inert, the potential involvement of AuNPs in epigenetic modifications was shown by several recent studies.[3,8–10] Hence, the development of effective testing strategies can help us to distinguish between adverse health effects of NMs exposure in contrast to adaptive changes.[11] Several NMs exhibited epigenetic effects in terms of deregulation of microRNA (miRNA) expression profiles.[11] miRNAs are small (typically 20–26 nucleotides), highly conserved single stranded non-coding RNA (ncRNA) molecules involved in the post-transcriptional regulation of gene expression that is related to nearly all developmental and pathological processes in animals.[12] MiRNAs are critical regulators of gene expression through acting as a guide by base-pairing with complementary sequences in target mRNA to negatively regulate its expression.[13] miRNAs participate in almost all known cellular processes including cell proliferation, differentiation, survival, metabolism, genome stability, apoptosis and inflammation.[14] Deregulation of miRNA has been shown to be broadly involved in a diverse range of pathological conditions such as cancer, cardiovascular and autoimmune diseases, mental disorders, and many more.[15,16] miRNA-155 is a typical multifunctional miRNA that is involved in numerous biological processes including hematopoiesis, inflammation, immunity and carcinogenesis.[17] miRNA-155 has been reported to be involved in the regulation of the level of expression of *TP53INP1* and *PROS1* genes.[9,18] *TP53INP1* gene is a tumor suppressor gene that encodes the anti-proliferative, pro-apoptotic and pro-autophagic protein; TP53INP1. It is a stress-induced p53- target gene that induces cell growth arrest and apoptosis by modulating p53 transcriptional activity.[19] The *PROS1* gene encodes for protein S (PS), a vitamin K-dependent plasma glycoprotein that functions as natural anticoagulant protein.[20] PS has been reported to be synthesized and secreted mainly in hepatocytes and other cells than hepatocytes like lung where it has the highest expression of PS.[9] Lack of protein S synthesis can lead to coagulopathy such as venous thrombosis giving rise to dire consequences.[21]

Biodistribution studies have identified the lung as one of the target sites of accumulation for AuNPs, necessitating further studies into their effects in the lung.[22,23] Thus, the current study, which is considered the first, was conducted to assess the effect of a single IV injection of AuNPs (0.015 mg Au/kg body wt) on the rat lung through the evaluation of its epigenetic effects regarding the *miR-155* and two of its putative target genes, *TP53INP1* and *PROS1*.

Materials and methods

Materials

A citrate-capped spherical gold nanoparticles (AuNPs) in aqueous solution, pink in color, with an average diameter size of 25±3 nm and 197 µg/ml concentration was purchased from NanoTech Egypt for Photo-Electronics Co., where they have been prepared by chemical reduction method as reported by Turkevich et al[24]. A drop of the purchased concentrated stock AuNPs solution was mounted on Formvar-coated copper grids and allowed to dry then viewed using a transmission electron microscope (TEM) (JEOL TEM, JEM-1230, Japan). The image confirmed the morphology and the diameter of the AuNPs (Figure 1).

Experimental animals and ethical approval

Thirty-two adult male Wister rats (*Rattus Norvegicus*) (~200 g each) were housed in humidity and temperature-controlled ventilated cages on a 12 h day/night cycle with a rodent diet and water provided ad libitum.

Experimental design and treatment

To conduct IV injections, AuNPs were further diluted (7.3 times) using ultra-pure water resulting in a mass concentration of 30 µg/ml. Rats were anesthetized by IP injection of Ketamine/Xylazine mixture (Ketamine: 80–100 mg/Kg; Xylazine: 10–12.5 mg/Kg) during AuNPs administration. A single tail-vein injection of 0.1 ml AuNPs (30 µg/ml) was

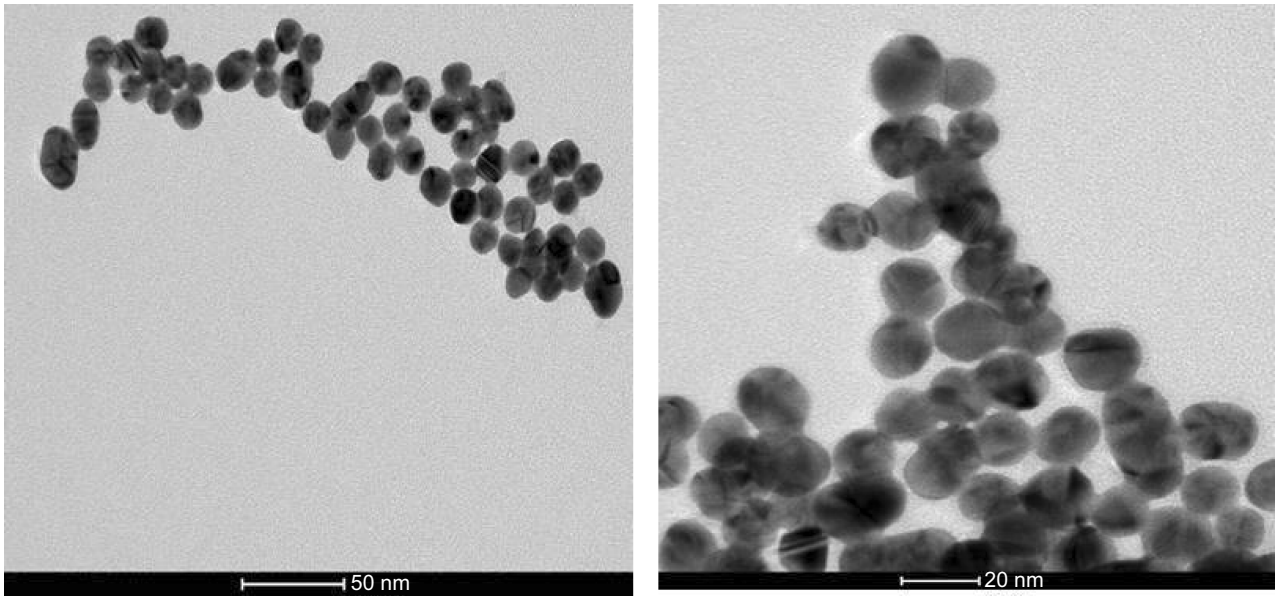

Figure 1 Characterization of AuNPs by transmission electron microscope (TEM): TEM micrographs of AuNPs showed the presence of dark-colored spherical nanoparticles of high atomic mass within the size range 25±3.

administrated slowly to the rats. The chosen dose (0.015 mg Au/kg body wt) used in this study is more relevant from a "normal" environmental exposure standpoint.[25] The selected AuNPs diameter size (25±3 nm) in the current study was due to the easy cellular uptake of spherical AuNPs with diameters between 20 and 30 nm.[26] Rats were randomly divided into two equal groups: the injected (n=16) and the vehicle-injected control group that was injected with equal amount of ultrapure water to serve as an internal control (n=16). Animals were then sacrificed at four time points (4 injected and 4 control animals/time point): one day, one week, one month and two months AuNP injection.

Sampling

Rats were euthanized by cervical dislocation at the stated time points and lungs were then collected and thoroughly washed with water to minimize adherent AuNPs, snap frozen in liquid nitrogen and stored at −80°C until analysis.

Transmission electron microscopy (TEM)

Random lung samples, harvested at one day post-injection, were used to confirm AuNPs delivery.[25] Tissue specimens were fixed in 2.5% glutaraldehyde for 1 h followed by post-fixation with 1% osmium tetroxide and potassium ferrocyanide (Sigma) for 1 h at room temperature. The samples were then dehydrated in an ascending series of ethanol before they were embedded in araldite (Sigma). Ultrathin sections were cut and mounted on Formvar-coated copper grids where they were doubly stained with uranyl acetate (BDH) and lead citrate (BDH) and viewed under a JEOL transmission electron microscope (JEM-1230, Japan), the most common method for AuNPs visualization.[2] Elemental analysis was performed using the JEOL EDX (Energy Dispersive X-ray) microanalysis unit coupled with a JEM-1230 electron microscope.

Quantitative real-time RT-PCR of MiRNA-155

Total miRNAs were isolated using mirVana™ miRNA Isolation Kit (Ambion, Ltd., Cambridgeshire, UK cat. no. AM1560) according to the manufacturers' instructions. Concentrations and purity of miRNA samples were assayed by electrophoresis and spectrophotometry by Nanodrop (ND-1000 Spectrophotometer, Thermo Scientific) and were diluted to 20 ng/µl. Mature *miR-155* expression was assessed by qRT-PCR according to the TaqMan® microRNA Assays protocol (Applied Biosystems, cat. no. 4427975) by the use of *U87* small nucleolar RNA (snoRNA) for normalization (Applied Biosystems). It is a two-step protocol requiring reverse transcription with miRNA-specific primer (provided in each assay), followed by real time PCR with TaqMan probes (provided in each assay). Primers and probes were synthesized by Applied Biosystems. The highly stable interaction between the MGB (minor groove binder)-probes and the target increases

the Tm of the probe and therefore increases the specificity and sensitivity of the assay.[27] Purified total miRNA was subjected to RT using a TaqMan® microRNA Reverse Transcription Kit (Applied Biosystems, cat. no. 4366596) and sequence-specific RT primers for miR155 (assay ID: 002571) and U87 (assay ID: 001712) following the manufacturer's protocol. For Real time RT-PCR reactions, 1.33 µl of the produced RT product was amplified in 20-µl PCR reaction containing 10 µl TaqMan Universal PCR master Mix II (2x) with no UNG (Applied Biosystems, Gent, Belgium, cat. no. 4440043) and 1 µl TaqMan MicroRNA Assay Mix (sequence-specific primers/probes). The reactions were incubated in Prime Pro 48 Real Time PCR System (TECHNE, PRIMEPRO48, UK) in a 48-well optical plate at 95°C for 10 min, followed by 40 cycles of 95°C for 15 s and 60°C for 1 min. The real-time PCRs for miR155 and U87 were run in triplicate with an RT-negative control included in each batch of reactions. The amplified transcripts were quantified using the comparative CT method ($2^{-\Delta\Delta CT}$) as described previously.[28]

Quantitative real-time RT-PCR of PROS1 and TP53INP1

qPCR is widely used as the most reliable method for quantifying gene transcript levels because of its sensitivity, accuracy and specificity.[29] Total RNA was extracted from tissue specimens using the Total RNA extraction kit (GF1 TRE kit, Vivantis technologies, cat. no. GF-TR-050, Sdn. Bhd., Malaysia) following manufacturer's instructions. The purity and concentration of the isolated RNA were ascertained spectrophotometrically using Nanodrop ND-1000 Spectrophotometer (Thermo Scientific). RT-PCR was performed using RevertAid Reverse Transcriptase, 200 U/µl (Thermo scientific, Cat. No. EP044, USA) following the guidelines provided. The mRNA expression level of each gene was determined relative to two endogenous reference genes (*ACTB* and *GAPDH*) by a fluorescence-based real-time detection method with a fluorescent SYBR Green dye (Thermo Scientific, Cat. No. K0221, USA) according to manufacturer instructions. Primer sequences presented in Table 1 were designed using Primer 3 software.[30] Cycle threshold (Ct) values were quantified by the use of Prime Pro 48 Real Time PCR System equipped with sequence detection system software (Sequence Detection System, version 5.2.15; TECHNE, PRIMEPRO48, UK) in 48-well qPCR plate. The real-time thermal profile was set as follows: 95°C for 5 min (initial denaturation) and then 40 cycles of denaturation at 95°C for 15 s, annealing at 60°C for 20 s and extending at 72°C for 15 s. The fluorescence intensity was acquired at the annealing step of each amplification cycle and the specificity of the amplicons was checked by performing the "melting curve" analysis of all samples through one cycle of 95°C for 15 s, 55°C for 15 s and 95°C for 15 s. Each qRT-PCR was performed in triplicates with no template control (NTC) included in each experiment. The comparative $2^{-\Delta\Delta CT}$ method was used to calculate the relative transcription levels.[28]

Western blot analysis

Total protein was extracted from lung samples using NP-40 lysis buffer (150 mM NaCl, 1% Triton X-100, 50 mM Tris) added with phosphatase inhibitor, protease inhibitor and PMSF (Biospes, cat. no. BWR1022, China) which prevents the protein of interest from degradation. The protein concentration of the lysates was quantified by the Bradford protein assay.[31] Equal amounts of total protein (10 µg) from different samples were resolved by 10% sodium dodecyl sulfate polyacrylamide gel by electrophoresis (SDS-PAGE) before being

Table 1 Sequence of primer sets used for qRT-PCR analysis

Gene	Primer sequence	Accession Number	Product size
Protein S (PROS1)	Forward:-GAAAACACCTGTGCCCAACT Reverse:-TCACGAAGTGCAATCAGGAG	NM_031086.2	323
Tumor protein P53 induced nuclear protein 1 (TP53INP1)	Forward:-GAGTCCTGTCCAATGGAGGA Reverse:-GCTGCAACACAGCAGTGAAT	NM_181084.2	260
Glyceraldehyde-3-phosphate dehydrogenase (GAPDH)	Forward:-ACCACAGTCCATGCCATCAC Reverse:-TCCACCACCCTGTTGCTGTA	NM_017008.4	452
Beta-actin (ACTB)	Forward:-TGTCACCAACTGGGACGATA Reverse:-GGGGTGTTGAAGGTCTCAAA	NM_031144.3	165

Notes: Primer sets designed using the free online software Primer3 (v. 0.4.0) http://bioinfo.ut.ee/primer3-0.4.0/: Copyright (c) 1996, 1997, 1998, 1999, 2000, 2001, 2004, 2006, 2007. Whitehead Institute for Biomedical Research, Steve Rozen, Maido Remm, Triinu Koressaar and Helen Skaletsky. All rights reserved.

transferred to polyvinylidene difluoride (PVDF) membranes (Bio-Rad) using the mini trans-blot system for detection. The membranes were blocked in 1% bovine serum albumin (BSA) in phosphate buffered saline (PBS) for 1 h and washed in PBS/0.02% Tween 20. Primary antibodies (polyclonal anti-protein S antibodies, Biospes, cat. no. YPA1300, China) were then added (1:100) to allow hybridizing to their respective specific proteins. Following an overnight incubation at 4°C, secondary horseradish peroxidase (HRP)-labeled goat anti-Rabbit IgGs (Biospes, cat. no. BSA1013, China) were added (1:1000) and membranes were incubated for 1 hr. The targeted protein bands were then developed at 75 KDa (PS) using DAB Horseradish Peroxidase Chromogenic Kit (Biospes, cat. no. BWR1069, China). The band intensities were quantified by densitometry using my image analysis software v.2.0 (Thermo scientific).

Statistical analysis

The data of experimental results were expressed as mean ± standard error (SEM). The differences in data of the groups were analyzed using independent samples two-way analysis of variance (ANOVA) by SPSS for Windows version 17.0 (IBM SPSS, Armonk, NY, USA). The value of $P<0.05$ is considered statistically significant.

Results

Charachterization of AuNPs

The morphology and size of AuNPs were characterized by TEM. AuNPs were spherical in shape with an average diameter size of 25±3 nm (Figure 1A and B).

Cellular uptake of AuNPs into lung cells

Cellular uptake of AuNPs into lung cells was confirmed using TEM where AuNPs frequently appeared as dark dense clusters enclosed by cytoplasmic vesicles or scattered in the cytosol (Figure 2A). Elemental analysis verified that the electron dense aggregates were AuNP as indicated by the two peaks corresponding to the gold M shell (2.2 KeV) and L shell (9.7 KeV) (Figure 2B). The observed copper peaks were due to the use of copper grids for sample mounting.

Modulation of miR-155 induced by AuNP exposure

The exposure to AuNPs resulted in a significant up-regulation in level of the expression of *miR-155* by 1.07 fold at one day post-injection of AuNPs. In contrast, the AuNPs injection causes a significant decrease in the expression level of

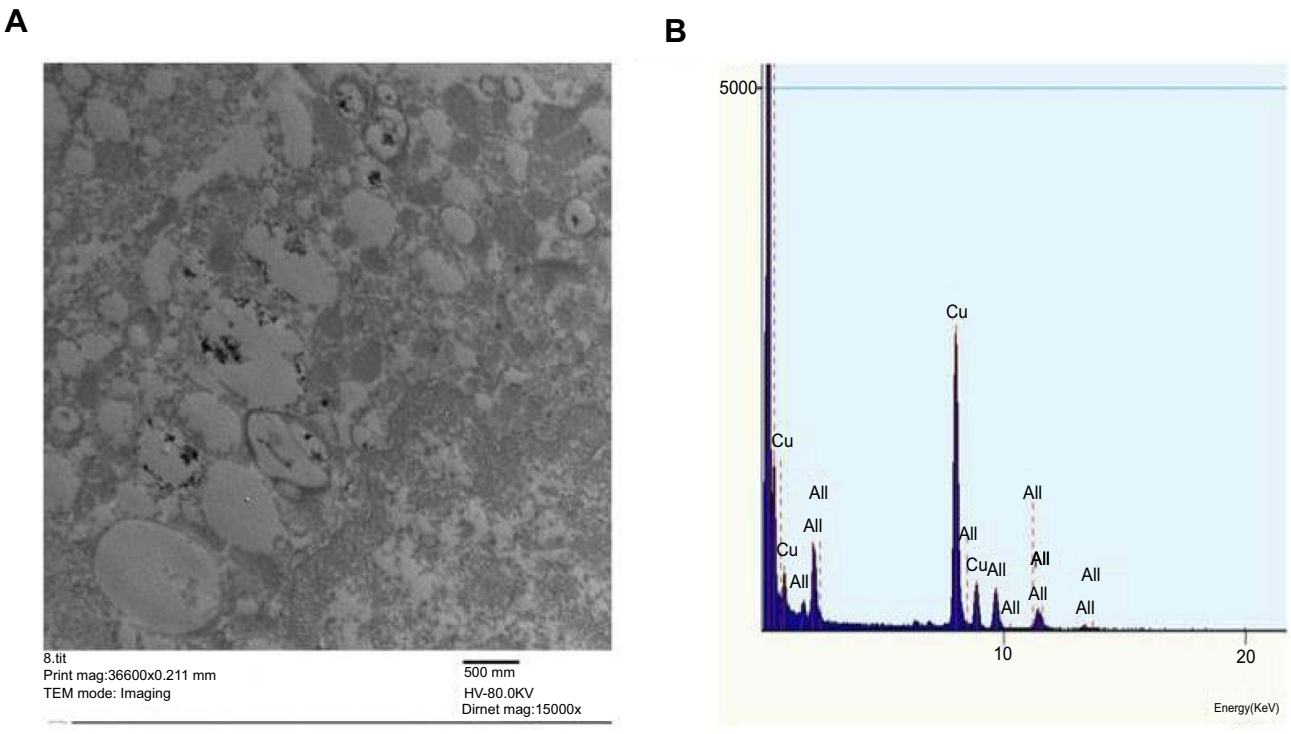

Figure 2 Ultrastructural localization of AuNPs in lung cells at one day post-injection of AuNPs: (**A**) TEM micrograph showing the cellular uptake of AuNPs by lung cells that were localized predominantly as electron dense clusters enclosed within the endosomes. Magnification: 36600X. Scale bar: 500 nm (**B**) EDX elemental analysis confirmed the presence of Au as depicted by two sharp peaks at 2.121 keV (AuL) and 9.712 keV (AuM).

miR-155 by 2.6, 10 and 16.7 folds at one week, one month and two months post-injection, respectively (Figure 3).

Expression of TP53INP1 and PROS1 genes

The AuNPs caused the *TP53INP1* expression level to be significantly decreased to 0.97 one day after the single IV injection. Meanwhile, the AuNPs significantly upregulated the expression of *TP53INP1* by 1.89, 3.4 and 1.18 folds one week, one month and two months after the AuNPs injection, respectively (Figure 4A). Moreover, our data revealed that AuNPs exposure induced a significant downregulation in *PROS1* expression by 2.3 folds at one day post-injection. In contrary, the AuNPs injection caused a significant elevation in the expression level of *PROS1* by 1.2, 1.45 and 1.67 folds

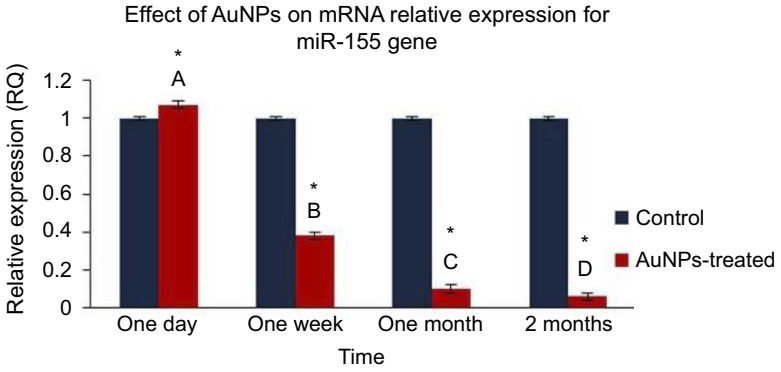

Figure 3 The effect of AuNPs exposure on mRNA relative expression level of *miR-155* gene: qRT-PCR results in lung tissue of rats at one day, one week, one month and two months post-injection of AuNPs. Data were expressed as means ± SEM (n=4) of triplicate experiments. Groups having different letters are significantly different from each other at $p<0.05$. Groups having (*) are significantly different compared with their control groups at $p<0.05$.

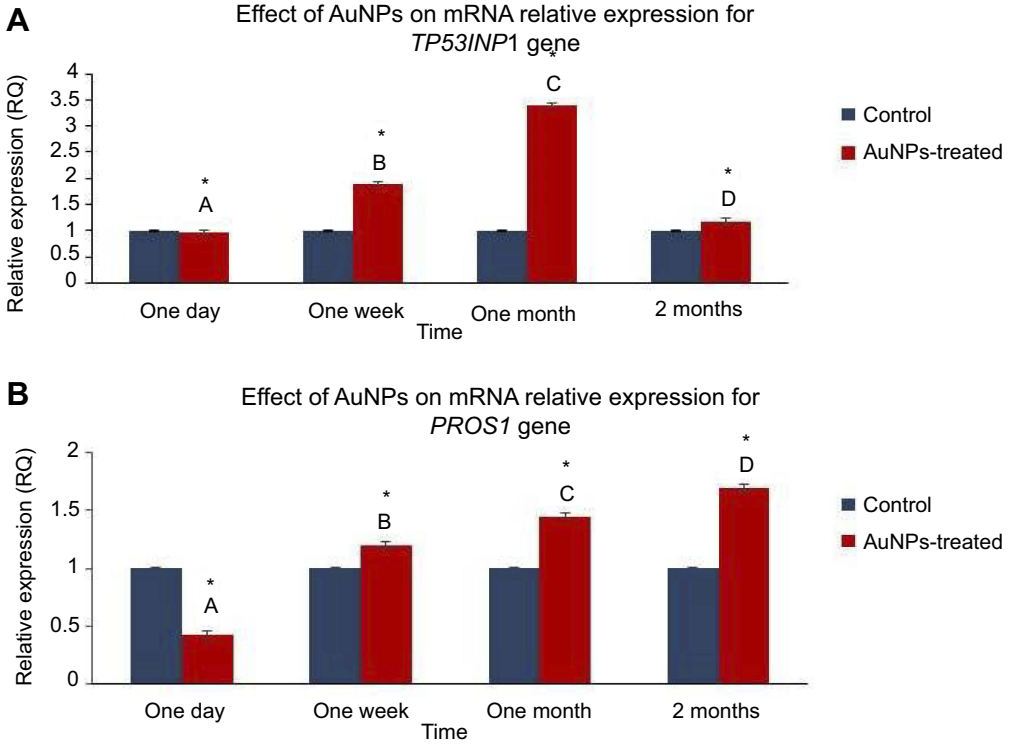

Figure 4 The effect of AuNPs exposure on the mRNA expression level of the *PROS1* and *TP53INP1* genes: qRT-PCR results in lung tissue of rats at one day, one week, one month and two months post-injection of AuNPs. (**A**) The mRNA relative expression of *TP53INP1* gene; (**B**) mRNA relative expression of *PROS1* gene. Data were expressed as means± SEM (n=4) of triplicate experiments. Groups having different letters are significantly different from each other at $p<0.05$. Groups having (*) are significantly different compared with their control groups at $p<0.05$.

at one week, one month and two months post-injection of AuNPs, respectively (Figure 4B).

Expression level of PS

The expression levels of PS were analyzed by Western blot analysis of protein samples of both control and AuNPs-treated groups (Figure 5A). The protein samples of lungs from rats after one day of AuNPs exposure exhibited significantly lower PS expression compared with their control group at the same time point (Figure 5B). However, the protein samples of lungs from rats after one week and one month of AuNPs exposure revealed significantly higher PS expression compared with their corresponding control group at the same time points (Figure 5B). Meanwhile, there was no significant variation in PS level between protein samples of the rat lung two months after the AuNPs injection and their corresponding control at the same time point (Figure 5B).

Discussion

Nanomedicine is an emerging field which provides a better understanding of disease mechanisms and supports more precise and rapid diagnosis, targeted and effective drug delivery and follows up of diseases.[3] Thus considering the effects of NMs administration is of great impact for their future usage in various applications. Epigenetic studies are fundamental in the safety assessment of nanoparticles. However, our understanding of the influence of NM exposure on the epigenome and its contribution to the development of diseases is far from complete. Choi et al were the first researchers who reported that NMs can cause significant epigenetic toxicity.[32] MiRNAs are becoming more crucial in understanding disease diagnosis and prognosis due to their role in gene expression and regulation.[33] Despite the possible epigenetic toxicity induced by AuNPs exposure, only a few studies have explored miRNA responses toward their administration. In fact, miR-155 epigenetic alterations have rarely been studied. These premises prompted us to explore alterations in *miR-155* expression and two of its putative target genes, *TP53INP1* and *PROS1* genes, in response to AuNPs exposure in the lung of a rat model.

The increased human exposure to AuNPs via the IV injection in the clinical applications necessitates the identification of hazards of AuNPs IV injection. It has been

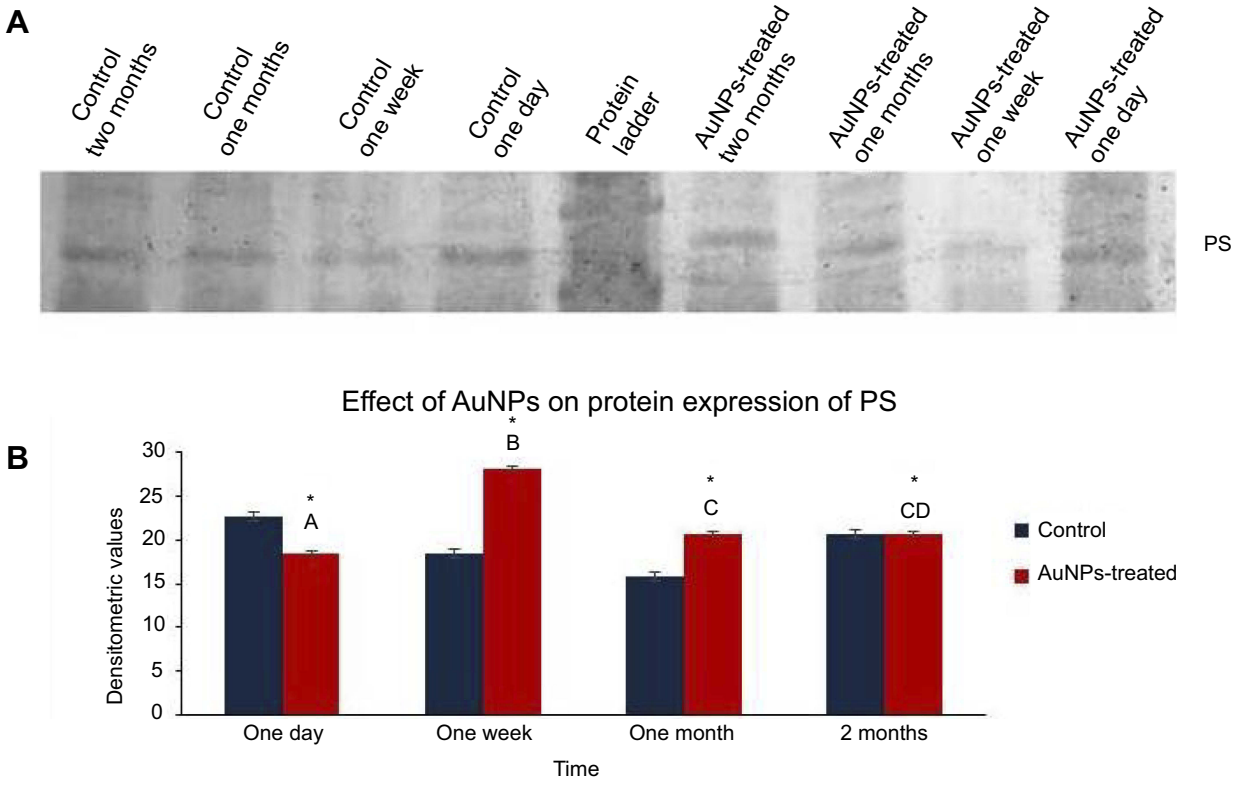

Figure 5 The effect of AuNPs exposure on the expression level of PS: Western blot analysis performed with antibodies against PS at one day, one week, one month and two months post-injection of AuNPs in lung tissue of rats. (**A**) A representative image of the PVDF membrane of Western blot analysis showed protein bands of PS at the expected size of 75 KDa; (**B**) Graphical representation showed the densitometric quantitation of the Western blot band intensities of PS. Data were expressed as means ± SEM (n=4) of triplicate experiments. Groups having different letters are significantly different from each other at $p<0.05$. Groups having (*) are significantly different compared with their control groups at $p<0.05$.

reported that the IV route had the lowest toxicity compared to the oral and IP routes.[34] Moreover, biodistribution studies have demonstrated the presence of AuNPs in various organs after IV injection where AuNPs were mainly accumulated in the liver, lungs and in the spleen.[22] It is noteworthy that AuNPs has been observed to reach lung via the systemic blood circulation in rats where levels of Au reach the maximum 2–3 hr after IV injection.[23,25] In an agreement, our results confirmed the cellular uptake of AuNPs into lung cells after IV administration where AuNPs were frequently detected as dark dense clusters enclosed by cytoplasmic vesicles under TEM possibly due to inherent properties such as high surface activity and high diffusivity.[35,36]

One miRNA could potentially control the expression of a few to several thousand genes. Conversely, each mRNA could be affected by multiple miRNAs.[37] MiRNAs recognize and bind their mRNA targets via extensive or partial Watson–Crick pairing of the microRNA seed sequence (nucleotides 2–8 of the microRNA) with a complementary sequence typically at the 3′untranslated region (3′-UTR) of its target mRNA where they degrade the targets and/or inhibit their translation, down-regulating protein expression.[38] MiR-155 was first identified as the product of the B-cell integration cluster (*bic*) gene, a frequently up-regulated gene in B-cell lymphoma.[39] Deregulation of miR-155 was reported to be associated with human lung cancer and during pulmonary fibrosis.[40,41]

Our RT-PCR analysis using the TaqMan probe and U87 snoRNA as endogenous reference gene revealed the presence of a relatively significant alteration in *miR-155* expression after AuNPs injection compared to controls. Moreover, miRNAs changes were still observed until two months after IV administration, indicating long-term effects of exposure to AuNPs. This is consistent with several studies showing the involvement of miRNAs in response to AuNPs exposure. A single IV injection of AuNPs in Wister rats induced up- and downregulation of 21 miRNAs in the peripheral blood both 1 week and 2 months post injection. Of these, miR-494, which binds to different sites in *PROS1* mRNA and regulates PS expression, was confirmed to be increased at 2 months post injection by 2 folds.[8,42] Moreover, 28 miRNAs were reported to be up-regulated in the fetal lung of mice treated with PEG-coated AuNPs.[10] In our study, the increased *miR-155* expression in the lung one day after the AuNPs exposure is concurrent with Ng et al who showed an increased expression of *miR-155* in human lung fibroblasts after exposure to AuNPs.[9] There appears to be a lack of data on rat lung *miR-155* after AuNPs exposure for comparison with our study. To our knowledge, this is the first report that AuNPs can affect the expression of *miR-155* in rat lung.

To investigate the molecular mechanism regarding *miR-155* alteration, we measured the relative mRNA expression levels of two of its putative target genes, *TP53INP1* and *PROS1* genes. *TP53INP1* gene is localized to rat chromosome 5q13 and encodes TP53INP1 which upon severe DNA damage, in association with homeodomain-interacting protein kinase-2 (HIPK2), phosphorylate p53 at Ser-46, enhancing P53 stability and transcriptional activity by promoting the binding of p53 to the promoter regions of apoptosis related genes leading to cell growth arrest and apoptosis.[19]

Our findings revealed the correlation of *miR-155* expression with the expression of its target gene; *TP53INP1*. It was demonstrated that the down-regulation in the expression of *TP53INP1* at one day post-injection of AuNPs was parallel with the up-regulation in expression of *miR-155*. Meanwhile, the elevated expressions of *TP53INP1* at one week, one month and two months post-injection of AuNPs were coupled with the decreased expressions of *miR-155* during these time points. This elevated expression of *TP53INP1* can result in enhancement of cell apoptosis and diminishing of cell proliferation. In agreement, the induction of apoptosis has been reported upon exposure to several NPs such as administration of titanium oxide (TiO_2) NPs that was involved in inducing apoptosis in the liver of Wister rats.[43] Moreover, it has been reported that in vitro exposure to 20 nm AuNPs in a tissue culture model of mouse retina can result in significantly higher number of apoptotic cells.[44] Furthermore, qRT- PCR results showed up-regulation of mRNA level of four pro-apoptotic genes combined with downregulation of one anti-apoptotic gene in human breast epithelial MCF-7 cells exposed to AuNPs.[45] In addition, the antitumor and apoptotic action of AuNPs in human liver carcinoma cell was reported through downregulation of anti-apoptotic and up-regulation of pro-apoptotic proteins.[46] In regard to anti-proliferative effect of AuNPs, It was proved that spherical and rod-shaped AuNPs were able to reduce cell proliferation of cancer cells in vitro.[47] There is a scarcity of data on rat lung *TP53INP1* expression and its pro-apoptotic and anti-proliferative effect after AuNPs or any other type of NMs exposure for comparison with this study.

The *PROS1* gene spans rat chromosome 7 and encodes for PS, a vitamin K-dependent plasma glycoprotein that function as natural anticoagulant protein at the crossroads of multiple biological processes, including coagulation, regulation of

inflammatory cytokine release, apoptosis, atherosclerosis, angiogenesis/vasculogenesis, and cancer progression.[20] The resulted RT-PCR data in this study revealed strong parallelism in alteration of *miR-155* and its target gene, *PROS1*. At one day post-injection of AuNPs, the down-regulation of *PROS1* expression was concomitant with the up-regulation of *miR-155*. Meanwhile, the elevation of the expression of *PROS1* at one week, one month and two months post-injection was coupled with the decrease in *miR-155* expression during the mentioned time points. To further explore whether AuNPs exposure modulates expression level of PS, Western blot analysis, the most commonly used laboratory techniques for identifying proteins, was conducted to measure the difference in PS level in AuNPs-treated groups compared to their control groups.[48] The Western blot analysis data demonstrated that PS expression level was mirrored to their corresponding *PROS1* mRNA levels at one day, one week and one month post –injection of AuNPs. These findings indicated that alteration of *miR-155* expression during those time points led to modulation of PROS1 at both the transcript and protein levels. Meanwhile, it is noteworthy to mention that there was a clear variation between the level of *PROS1* mRNA and PS level at two months post-injection where the *PROS1* mRNA was elevated but PS level remained constant compared with the control group. This finding comes in the same line with other report showing that a gene mRNA expression level and its protein level could be not mirrored to each other.[49] There are only a few reports on the involvement of PS expression in relation to AuNP-induced effects. Concurrent with another report, up-regulation of *miR-155* was observed concomitant with down-regulation of the *PROS1* gene and protein.[9] It has been reported that PS deficiency can contribute to thrombosis in the pulmonary vasculature, causing pulmonary hypertension and lung infarction culminating in death.[50,51] Therefore, modulation of *PROS1* by miR-155 has a clinical significance and can shed light on a link between AuNPs exposure and PS deficiency associated diseases. Modification of PS level, a component of the hemostatic system, may have effects on the development of thrombosis or hemorrhage.[52] This hypothesis is consistent with another study which established that exposure to AgNPs and silica NPs enhanced venous thrombus formation and platelet aggregation.[53,54] We propose that more studies on the involvement of AuNPs with thrombosis must be conducted.

Conclusion

In this report, the principal finding referred to the identification of miR-155 as a deregulated miRNA in response to a single IV injection of AuNPs in rat lung in terms of both acute and chronic administration. It was revealed that the miR-155 and its putative target genes, TP53INP1 and PROS1have characteristic expression patterns that persisted up to two months post-exposure to the AuNPs. However, we propose that more studies on the biochemical mechanisms related to the administration of different doses and sizes of AuNPs on the lung tissues may be conducted.

Abbreviation list

AuNPs, Gold nanoparticles; miR-155, microRNA-155; TP53INP1, Tumor protein 53 inducible nuclear protein 1; PROS1, Protein S gene; PS, Protein S; NMs, Nanomaterials; nc-RNA, Non-coding RNA; TEM, Transmission Electron Microscope; EDX, Energy Dispersive X-ray; snoRNA, Small nucleolar RNA; GAPDH, Glyceraldehyde-3-phosphate dehydrogenase; ACTB, Beta-actin; SDS-PAGE, Sodium dodecyl sulfate polyacrylamide; PVDF, Polyvinylidene difluoride; BSA, Bovine serum albumin; PBS, Phosphate buffered saline; HRP, Horseradish peroxidase; SEM, mean ± Standard error; ANOVA, Analysis of variance; 3'-UTR, 3'untranslated region; HIPK2, Homeodomain-interacting protein kinase-2; bic , B-cell integration cluster gene.

Ethics approval and consent to participate

All procedures involving animals were carried out according to the Institutional Animal Care and Use Committee (IACUC). The local Committee for the Faculty of Veterinary Medicine, Cairo University approved the design of the experiment and the protocol with the approval number (CU/II/F/42/17).

Data availability

The datasets generated and/or analyzed during the current study are available from the corresponding author on reasonable request.

Acknowledgments

This research did not receive any specific grant from funding agencies in the public, commercial, or not-for-profit sectors.

Disclosure

The authors declare that they have no competing interests in this work.

References

1. Rosa S, Connolly C, Schettino G, et al.. Biological mechanisms of gold nanoparticle radiosensitization. *Cancer Nano*. 2017;8:2. doi:10.1186/s12645-017-0026-0
2. Panzarini E, Mariano S, Carata E, et al. Intracellular transport of silver and gold nanoparticles and biological responses: an update. *Int J Mol Sci*. 2018;19(5):1305. doi:10.3390/ijms19051305
3. Smolkova B, Dusinska M, Gabelova A. Nanomedicine and epigenome. Possible health risks. *Food Chem Toxicol*. 2017;109:780–796. doi:10.1016/j.fct.2017.07.020
4. Murali K, Neelakandan MS, Thomas S. Biomedical applications of gold nanoparticles. *JSM Nanotechnol Nanomed*. 2018;6(1):1064.
5. Marczylo EL, Jacobs MN, Gant TW. Environmentally induced epigenetic toxicity: potential public health concerns. *Crit Rev Toxicol*. 2016;46(8):676–700. doi:10.1080/10408444.2016.1175417
6. Shyamasundar S, Ng CT, Yung LY, et al. Epigenetic mechanisms in nanomaterial-induced toxicity. *Epigenomics*. 2015;7(3):395–411. doi:10.2217/epi.15.3
7. Smolkova B, El Yamani N, Collins AR, Gutleb AC, Dusinska M. Nanoparticles in food. Epigenetic changes induced by nanomaterials and possible impact on health. *Food Chem Toxicol*. 2015;77:64–73. doi:10.1016/j.fct.2014.12.015
8. Chew WS, Poh KW, Siddiqi NJ, et al. Short and long-term changes in blood miRNA levels after nanogold injection in rats–potential biomarkers of nanoparticle exposure. *Biomarkers*. 2012;17(8):750–757. doi:10.3109/1354750X.2012.727030
9. Ng CT, Dheen ST, Yip WC, et al. The induction of epigenetic regulation of PROS1 gene in lung fibroblasts by gold nanoparticles and implications for potential lung injury. *Biomaterials*. 2011;32(30):7609–7615. doi:10.1016/j.biomaterials.2011.06.038
10. Balansky R, Longobardi M, Ganchev G, et al. Transplacental clastogenic and epigenetic effects of gold nanoparticles in mice. *Mutat Res*. 2013;751-752:42–48. doi:10.1016/j.mrfmmm.2013.08.006
11. Dusinska M, Tulinska J, El Yamani N, et al. Immunotoxicity, genotoxicity and epigenetic toxicity of nanomaterials: new strategies for toxicity testing? *Food Chem Toxicol*. 2017;109(Pt 1):797–811. doi:10.1016/j.fct.2017.08.030
12. Ha M, Kim VN. Regulation of microRNA biogenesis. *Nat Rev Mol Cell Biol*. 2014;15(8):509–524. doi:10.1038/nrm3838
13. Kotipalli A, Gutti R, Mitra CK. Dynamics of miRNA biogenesis and nuclear transport. *J Integr Bioinform*. 2016;13(5):305. doi:10.2390/biecoll-jib-2016-305
14. Masud MK, Umer M, Hossain MShA, et al. Nanoarchitecture frameworks for electrochemical miRNA detection. *Trends Biochem Sci*. 2019;44(5):433–452. doi:10.1016/j.tibs.2018.11.012
15. Esteller M. Non-coding RNAs in human disease. *Nat Rev Genet*. 2011;12(12):861–874. doi:10.1038/nrg3074
16. Paul P, Chakraborty A, Sarkar D, et al. Interplay between miRNAs and human diseases. *J Cell Physiol*. 2017;233(3):2007–2018. doi:10.1002/jcp.25854
17. Faraoni I, Antonetti FR, Cardone J, et al. MiR-155 gene: A typical multifunctional microRNA. *Biochim Biophys Acta*. 2009;1792(6):497–505. doi:10.1016/j.bbadis.2009.02.013
18. Zhang J, Cheng C, Yuan X, et al. microRNA-155 acts as an oncogene by targeting the tumor protein 53-induced nuclear protein 1 in esophageal squamous cell carcinoma. *Int J Clin Exp Pathol*. 2014;7(2):602–610.
19. Shahbazi J, Lock R, Liu T. Tumor Protein 53-induced nuclear protein 1 enhances p53 function and represses tumorigenesis. *Front Genet*. 2013;4:80. doi:10.3389/fgene.2013.00080
20. Suleiman L, Négrier C, Boukerche H. Protein S: a multifunctional anticoagulant vitamin K-dependent protein at the crossroads of coagulation, inflammation, angiogenesis, and cancer. *Crit Rev Oncol Hematol*. 2013;88(3):637–654. doi:10.16/j.critrevonc.2013.07.004
21. Lijfering WM, Mulder R, ten Kate MK, et al. Clinical relevance of decreased free protein S levels: results from a retrospective family cohort study involving 1143 relatives. *Blood*. 2009;113(6):1225–1230. doi:10.1182/blood-2008-08-174128
22. Bednarski M, Dudek M, Knutelska J, et al. The influence of the route of administration of gold nanoparticles on their tissue distribution and basic biochemical parameters: in vivo studies. *Pharmacol Re*. 2015;67(3):405–409. doi:10.1016/j.pharep.2014.10.019
23. Isseia T, Shoa N, Naotoa O, et al. Biodistribution and excretion of colloidal gold nanoparticles after intravenous injection: effects of particle size. *Biomed Mater Eng*. 2017;28(3):315–323. doi:10.3233/BME-171677
24. Turkevich J, Stevenson PC, Hillier J. A study of the nucleation and growth processes in the synthesis of colloidal gold. *Discuss Faraday Soc*. 1951;11:55–75. doi:10.1039/DF9511100055
25. Balasubramanian SK, Jittiwat J, Manikandan J, et al. Biodistribution of gold nanoparticles and gene expression changes in the liver and spleen after intravenous administration in rats. *Biomaterials*. 2010;31(8):2034–2042. doi:10.1016/j.biomaterials.2009.11.079
26. Chen H, Dorrigan A, Saad S, et al. In vivo study of spherical gold nanoparticles: inflammatory effects and distribution in mice. *PLoS One*. 2013;8(2):e58208. doi:10.1371/journal.pone.0058208
27. Navarro E, Serrano-Heras G, Castaño MJ, Solera J. Real-time PCR detection chemistry. *Clinica Chimica Acta*. 2015;439:231–250. doi:10.1016/j.cca.2014.10.017
28. Livak KJ, Schmittgen TD. Analysis of relative gene expression data using real- time quantitative PCR and the 22DDCT. *Nat Methods*. 2001;25:402–408. doi:10.1006/meth.2001.1262
29. Bustin SA, Benes V, Garson JA, et al. The MIQE guidelines: minimum information for publication of quantitative real-time PCR experiments. *Clin Chem*. 2009;55:611–622. doi:10.1373/clinchem.2008.112797
30. Untergrasser A, Cutcutache I, Koressaar T, et al. Primer3 - new capabilities and interfaces. *Nucl Acids Res*. 2012;40(15):e115. doi:10.1093/nar/gks596
31. Bradford MM. A rapid and sensitive method for the quantitation of microgram quantities of protein utilizing the principle of protein-dye binding. *Analyt Biochem*. 1976;72:248–254. doi:10.1016/0003-2697(76)90527-3
32. Choi AO, Brown SE, Szyf M, Maysinger D. Quantum dot-induced epigenetic and genotoxic changes in human breast cancer cells. *J Mol Med (Berl)*. 2008;86(3):291–302. doi:10.1007/s00109-007-0274-2
33. Islam MN, Masud MK, Haque MH, et al. RNA biomarkers: diagnostic and prog-nostic potentials and recent developments of electrochemical biosensors. *Small Methods*. 2017;1:1700131. doi:10.1002/smtd.201700131
34. Zhang X, Wu HY, Wu D, et al. Toxicologic effects of gold nanoparticles in vivo by different administration routes. *Int J Nanomedicine*. 2010;5:771–781. doi:10.2147/IJN.S8428
35. Kim S, Choi JE, Choi J, et al. Oxidative stress-dependent toxicity of silver nanoparticles in human hepatoma cells. *Toxicol In Vitro*. 2009;23:1076–1084. doi:10.1016/j.tiv.2009.06.001
36. Gosens I, Post JA, de la Fonteyne LJ, et al. Impact of agglomeration state of nano- and submicron sized gold particles on pulmonary inflammation. *Part Fibre Toxicol*. 2010;7:37. doi:10.1186/1743-8977-7-37
37. Pillai RS. MicroRNA function: multiple mechanisms for a tiny RNA? *RNA*. 2005;11(12):1753–1761. doi:10.1261/rna.2248605
38. Bartel DP. MicroRNAs: target recognition and regulatory functions. *Cell*. 2009;136(2):215–233. doi:10.1016/j.cell.2009.01.002
39. Eis PS, Tam W, Sun L, et al. Accumulation of miR-155 and BIC RNA in human B cell lymphomas. *Proc Natl Acad Sci USA*. 2005;102(10):3627–3632. doi:10.1073/pnas.0500613102
40. Czubak K, Lewandowska MA, Klonowska K, et al. High copy number variation of cancer-related microRNA genes and frequent amplification of DICER1 and DROSHA in lung cancer. *Oncotarget*. 2015;6(27):23399–23416. doi:10.18632/oncotarget.4351

41. Pottier N, Maurin T, Chevalier B, et al. Identification of keratinocyte growth factor as a target of microRNA-155 in lung fibroblasts: implication in epithelial-mesenchymal interactions. *PLoS One*. 2009;4(8):e6718. doi:10.1371/journal.pone.0006718
42. Tay JW, Romeo G, Hughes QW, Baker RI. Micro-ribonucleic acid 494 regulation of protein S expression. *J Thromb Haemost*. 2013;11:1547–1555. doi:10.1111/jth.12331
43. Morgan A, Ibrahim MA, Galal MK, Ogaly HA, Abd-Elsalam RM. Innovative perception on using Tiron to modulate the hepatotoxicity induced by titanium dioxide nanoparticles in male rats. *Biomed Pharmacother*. 2018;103:553–561. doi:10.1016/j.biopha.2018.04.064
44. So¨derstjerna E, Bauer P, Cedervall T, et al. Silver and gold nanoparticles exposure to in vitro cultured retina – studies on nanoparticle internalization, apoptosis, oxidative stress, glial- and microglial activity. *PLoS One*. 2014;9(8):e105359. doi:10.1371/journal.pone.0105359
45. Selim ME, Hendi AA. Gold nanoparticles induce apoptosis in MCF-7 human breast cancer cell. Research communication. *Asian Pacific J Cancer Prev*. 2012;13(4):1617–1620. doi:10.7314/APJCP.2012.13.4.1617
46. De Araújo RF Jr, Pessoa JB, Cruz LJ, et al. Apoptosis in human liver carcinoma caused by gold nanoparticles in combination with carvedilol is mediated via modulation of MAPK/Akt/mTOR pathway and EGFR/FAAD proteins. *Int J Oncol*. 2018;52(1):189–200. doi:10.3892/ijo.2017.4179
47. Wozniak A, Malankowska A, Nowaczyk G, et al. Size and shape-dependent cytotoxicity profile of gold nanoparticles for biomedical applications. *J Mater Sci Mater Med*. 2017;28(6):92. doi:10.1007/s10856-017-5902-y
48. Ghosh R, Gilda JE, Gomes AV. The necessity of and strategies for improving confidence in the accuracy of Western blots. *Expert Rev Proteomics*. 2014;11(5):549–560. doi:10.1586/14789450.2014.939635
49. Kamel S, Ibrahim MA, Awad ET, El-Hindi HMA, Abdel-Aziz SA. Molecular cloning and characterization of the novel CYP2J2 in dromedary camels (Camelus dromedarius). *Int J Biol Macromol*. 2018;120(PtB):1770–1776. doi:10.1016/j.ijbiomac.2018.09.193
50. Piazza G, Goldhaber SZ. Chronic thromboembolic pulmonary hypertension. *N Engl J Med*. 2011;364(4):351–360. doi:10.1056/NEJMra0910203
51. Zander DS, Baz MA, Visner GA, et al. Analysis of early deaths after isolated lung transplantation. *Chest*. 2001;120(1):225–232. doi:10.1378/chest.120.1.225
52. Teruel-Montoya R, Rosendaal FR, Martinez C. MicroRNAs in hemostasis. *J Thromb Haemost*. 2015;13:170–181. doi:10.1111/jth.12788
53. Jun EA, Lim KM, Kim K, et al. Silver nanoparticles enhance thrombus formation through increased platelet aggregation and procoagulant activity. *Nanotoxicology*. 2011;5(2):157–167. doi:10.3109/17435390.2010.506250
54. Corbalan JJ, Medina C, Jacoby A, Malinski T, Radomski MW. Amorphous silica nanoparticles aggregate human platelets: potential implications for vascular homeostasis. *Int J Nanomedicine*. 2012;7:631–639. doi:10.2147/IJN.S28293